HHS Public Access

Author manuscript

Neuropeptides. Author manuscript; available in PMC 2019 October 01.

Published in final edited form as:

Neuropeptides. 2018 October ; 71: 97–103. doi:10.1016/j.npep.2018.06.003.

Clearance kinetics of the VGF-derived Neuropeptide TLQP-21

ZengKui Guo[1], **Bhavani Sahu**[2], **Rongjun He**[3], **Brian Finan**[3], **Cheryl Cero**[2], **Raffaello Verardi**[4], **Maria Razzoli**[2], **Gianluigi Veglia**[4], **Richard D. Di Marchi**[3], **John M. Miles**[1], and **Alessandro Bartolomucci**[2]

[1]Mayo Foundation, 200 First Street SW, Rochester, MN 55905

[2]Department of Integrative Biology and Physiology, University of Minnesota, Minneapolis, MN 55455

[3]Novo Nordisk Research Center Indianapolis, Indianapolis, Indiana, 46241, USA

[4]Department of Biochemistry, Molecular Biology and Biophysics, University of Minnesota, Minneapolis, MN 55455

Abstract

TLQP-21 is a multifunctional neuropeptide and a promising new medicinal target for cardiometabolic and neurological diseases. However, to date its clearance kinetics and plasma stability have not been studied. The presence of four arginine residues led us to hypothesize that its half-life is relatively short. Conversely, its biological activities led us to hypothesize that the peptide is still taken up by adipose tissues effectively. [^{125}I]TLQP-21 was *i.v.* administered in rats followed by chasing the plasma radioactivity and assessing tissue uptake. Plasma stability was measured using LC-MS. *In vivo* lipolysis was assessed by the palmitate rate of appearance. Results: A small single *i. v.* dose of [^{125}I]TLQP-21 had a terminal half-life of 110 minutes with a terminal clearance rate constant, k_t, of 0.0063/min, and an initial half-life of 0.97 minutes with an initial clearance rate constant, k_i, of 0.71/min. The total net uptake by adipose tissue accounts for 4.4% of the entire dose equivalent while the liver, pancreas and adrenal gland showed higher uptake. Uptake by the brain was negligible, suggesting that i.v.-injected peptide does not cross the blood-brain-barrier. TLQP-21 sustained isoproterenol-stimulated lipolysis *in vivo.* Finally, TLQP-21 was rapidly degraded producing several N-terminal and central sequence fragments after 10 and 60 minutes in plasma *in vitro.* This study investigated the clearance and stability of TLQP-21 peptide for the first time. While its pro-lipolytic effect supports and extends previous findings, its short half-life and sequential cleavage in the plasma suggest strategies for chemical modifications in order to enhance its stability and therapeutic efficacy.

Corresponding Author: Alessandro Bartolomucci, abartolo@umn.edu.

AUTHORHIP COTRIBUTIONS

Participated in research design: Guo, Finan, Di Marchi, Miles, Bartolomucci; Conducted experiments: Guo, Sahu, He, Cero, Verardi Razzoli; Contributed new reagents or analytic tools: Verardi, Veglia Performed data analysis: Guo, Sahu, He, Finan; Wrote or contributed to the writing of the manuscript: Guo, Sahu, Razzoli, Di Marchi, Miles, Bartolomucci

Keywords

Adipose tissue; pharmacokinetics; tissue uptake; lipolysis; isotopes; rats; Complement 3a receptor 1.

INTRODUCTION

TLQP-21 is a multifunctional neuropeptide derived from the proteolytic cleavage of the 617-aa VGF pro-petide by prohormone convertase (PC) 1/3 and PC2 [Bartolomucci et al., 2006, 2011; Trani et al., 1995]. TLQP-21 regulates energy balance [Bartolomucci et al., 2006, Jethwa et al., 2007; Possenti et al., 2012; Cero et al., 2017], islet biology [Stephens et al., 2012, 2017; Petrocchi-Passeri et al., 2015], gastric function [Severini et al., 2009], nociception [Rizzi et al., 2008; Fairbanks et al., 2014; Doolen et al., 2017], blood pressure regulation [Fargali et al., 2014], reproduction [Aguilar et al., 2013], and stress [Razzoli et al., 2012]. The best characterized biological role of TLQP-21 reported to date is opposing obesity when administered centrally or peripherally by a mechanism largely mediated through activation of the complement 3a receptor (C3aR1) [Cero et al., 2014, 2017. See also Hannedouche et al., 2012; Cassina et al., 2013; Molteni et al., 2017]. When chronically administered intracerebroventricularly, TLQP-21 prevents obesity by increasing energy expenditure and heat production in mice fed a high fat diet without altering food intake [Bartolomucci et al., 2006], and decreases gastric emptying in rats [Severini et al., 2009]. Recently, it has been shown that TLQP-21 increases isoproterenol-induced lipolysis in murine adipose tissue and cultured adipocytes in a dose-dependent manner [Possenti et al., 2012; Cero et al., 2014, 2017]. Therefore, a growing body of evidence suggests that TQLP-21 is a potent pharmacological candidate for the treatment of obesity. On the other hand, relatively little is known currently about the clearance kinetics of TLQP-21. In the present study, we employed several pharmacokinetic approaches aimed to determine the clearance and tissue distribution of TLQP-21 related to its pro-lipolytic effects.

MATERIALS AND METHODS

The materials:

[^{125}I]TLQP-21 was synthesized as previously reported [Possenti et al., 2012; Cero et al., 2014]). [U-^{13}C]palmitate was purchased from Isotec (99% atom %, Sigma Chemicals, MO). After approval of the protocol by Mayo Animal Care and Use Committee and Mayo Radiation Safety, two series of experiments were performed in male Sprague Dawley rats fed a regular rodent chow diet (4.5% dietary fat). The experiments were conducted in the morning without prior fasting.

Clearance kinetics and tissue distribution of TLQP-21:

Rats (n=8, ~400 g) were acutely catheterized in a tail artery under local anesthesia in the morning, as described previously [Guo and Zhou 2003] for repeated arterial blood collections. After 30 min of recovery, an intravenous infusion line was installed in a lateral tail vein by transdermal venipuncture. The testing peptide, [^{125}I]TLQP-21 (6–10 μCi, specific activity ~0.25 μCi/μg), was injected into the infusion line followed by repeated

blood collections at 5 min intervals for 20 min to determine its clearance kinetics. Then, the rats were euthanized and various tissues were collected rapidly for the measurement of uptake of the peptide, bound and unbound.

Acute effect of TLQP-21 on lipolysis:

Tail arterial catheter and i *v.* infusion line were installed acutely as described above (n=8). After 30 min of recovery, constant *i. v.* infusion of [U-^{13}C]palmitate was started at 0.5 μmol•kg^{-1}•min^{-1}. After 20 minutes of equilibration, blood samples were collected at 5 min intervals for the measurement of basal lipolysis (plasma palmitate rate of appearance, Ra) using the steady state equation. Constant infusion of isoproterenol (30 ng•min^{-1}) was then started, 15 min into which either 40 μg ofTLQP-21 [Bartolomucci et al., 2006; Cero et al., 2017] or same volume of saline was injected *i. v.* as a bolus followed by periodic blood sampling for 60 min to determinate plasma palmitate concentration. The area under the curve (AUC) of plasma palmitate concentration and palmitate Ra were used to determine the effect of TLQP-21 on isoproterenol-stimulated lipolysis.

Mouse Plasma Stability Study Procedure:

TLQP-21 was incubated in 100% mouse plasma (100uL) at concentration at 1mM at 37°C for the duration of the study. At the time points of 0 min, 10 min, 30 min, and 60 min, aliquots of the incubated solutions were withdrawn (15uL) and diluted with 3x acetonitrile/ethanol mixture (v/v=l:l, 45uL) to precipitate the plasma proteins, and peptides were present in solution. The mixture was subsequently treated by microcentrifugation at 15,000 rpm for 2 min to remove the precipitation, the upper clear supernatant was collected and subjected to the LC-MS (Agilent Quadrupole 6120 LC-MS, ESI mode) analysis using a linear gradient of buffer B over buffer A (A: 100% water, 0.05% TFA; B: 90% aqueous acetonitrile, 0.05% TFA) on a Kinetex C8 column (2.6μM, 100Å, 75×4.6mm). The area under the curve of the peak at each time point was compared to the 0 min time point for calculating the percentage of the remaining peptide, and the degraded peptide products were studied by analyzing the Mass data of newly formed peaks.

Laboratory assays

[^{125}I]TLQP-21:

Plasma is isolated immediately upon collection onsite using a micro-centrifuge (Labnet International, Inc., Edison, NJ) and stored at −20°C. The gamma radioactivity (CPM) of [^{125}I]TLQP-21 in plasma is counted on a liquid scintillation counter, expressed as CPM/ml of plasma. Tissues tested as mentioned in Results are weighed on a gravity micro-balance, homogenized and a known amount is counted on the same LSC to determine CPM per gram of wet tissue. The results are normalized to CPM/g of wet tissue. Tissue protein content is determined using the Thermo Scientific™ Pierce™ BCA™ Protein assay (Fisher Scientific, Waltham, MA, USA) and used as the denominator for expressing the tissue radioactivity as CPM/ug of tissue protein. Note that the uptake presented here is the net amount without knowing the reversal (taken up and then released) which is not measured. Thus, the gross uptake (net uptake plus released) is assumed to be greater. On the other hand, it is this net

uptake, the amount of drugs actually accumulated in a given tissue, that likely determines the biological activity of the peptide.

Fatty acids:

Plasma is extracted for free fatty acids (FFA) using the Dole method [1956_] The extracted FFA are derivatized into the methyl ester as previously detailed [Guo et al., 1997], The methyl palmitate is analyzed on a single quadrupole GC-MS (Agilent, CA) and the concentration and the ^{13}C-enrichment of palmitate was calculated as previously described [Guo et al., 1997].

QPCR methods

RNA was obtained by homogenizing around 50–100 mg of frozen tissue in 500 ml of TRI REAGENT (Molecular Research Center, Inc., Cincinnati, Ohio) on ice following manufacturer's instructions. Total RNA was digested with DNase I using DNA-free (Ambion, Austin, TX) and tested for the presence of DNA contamination using PCR. Total RNA concentration and purity was then determined by spectrophotometer at 260 nm (NanoDrop 2000 UV-Vis Spectrophotometer, Thermo Scientific). 500 ng of RNA was converted into cDNA using iScript cDNA Synthesis Kit (Bio-Rad Laboratories, Hercules, CA) and relative quantification of mRNAs was performed with 3.5 μl of cDNA used in each 11.5 μl real-time-RT-PCR reaction using C1000 thermal cycler™ (Bio-Rad Laboratories, Hercules, CA). The PCR reactions were carried out using IQ™ Syber Green Supermix (BIO-RAD). Primers for the target genes are 5'ATC TGG CAC CAC ACC TTC 3', 5' AGC CAG GTC CAG ACG CA 3' for actin and 5' CAT GGG CGT ATA AAG GAC TGC 3', 5' GAA GCC TCC TAC TGT GCT CAT AG 3' for C3aRl. Thermal cycling parameters were as follows: an initial denaturing step (95 °C for 10 min), followed by 40 cycles of denaturing, annealing, and extending (95 °C for 45 s, 58 °C for 45 s and then 60 °C for 1 min, respectively) in a 96-well BioRad plate. The results were calculated by the comparative C_t method using β-actin as an endogenous reference gene, according to the Applied Biosystems ABI PRISM 7700 User Bulletin #2. The expression relative to β-actin was determined by calculating $2^{-\Delta Ct}$.

Statistical analysis

Data are presented as mean±SEM unless indicated otherwise. Non-paired Students' t-test is used for comparisons between two groups. For comparisons among three groups or more (e.g. different tissues or tissue parts), single-factor ANOVA analysis is utilized. Mean comparison was performed using the Turkey post hoc test. α value of 0.05 is used as the criteria for detecting statistical significance.

RESULTS

TLQP-21 clearance kinetics

Fig. 1 depicts the clearance kinetics of ^{125}I-TLQP-21 administered *i.v.* as a bolus (8.3 μCi. 40μg) in normally fed rats. The peptide is cleared from plasma exponentially *(inset)* as commonly seen with other drugs and peptides such as metformin [Choi et al., 2010; Gros et al., 1990; Adamet al., 2010; Wagner et al., 2016], The initial phase (by 1 min) shows a

clearance rate constant (k_i) of 0.40•min^{-1} and a half-life [$t_{1/2(i)}$] of 1.7 min. The extrapolated time-zero plasma radioactivity (Q_0) is an underestimate because the calculated plasma volume of distribution (17.6 ml) is much greater than the plasma volume reported for the rats of this size, i.e. ~12.5 ml [Davies and Morris 1993] When corrected for this discrepancy (i.e. by forcing the plasma volume to be 12.5 ml), the initial clearance rate constant is (k_i') is determined to be 0.71•min^{-1} with a half-life [$t_{i/2(i)}$'] of 0.97 min. At this clearance rate, 99% of the injected peptide is cleared in 6.4 min (i.e. in 6.6 half-lives), suggesting fast proteolysis or uptake by tissues.

The rapid initial clearance diminished exponentially, consistent with a multi-compartmental distribution kinetics for the peptide. After 8 min, the clearance curve had approached a steady state (pseudo-linearity) indicating the terminal phase. The terminal clearance rate constant (k_t) is 0.0063•min^{-1} with a half-life [$t_{1/2(t)}$] of 110 min. Based on this clearance rate, the mean residence time (MRT) for the peptide is calculated to be 159 min and its terminal volume of distribution (V_t) is 4258 ml•kg^{-1}. Using Q_0' (the corrected zero-time radioactivity) rather than Q_0 (the uncorrected) in calculating the AUC of plasma radioactivity (1.69•e^{8}CPM•ml^{-1}min^{-1}) for the interval of 0–726 min (726 min, the time point when 99% of the injected isotope would have been eliminated at the terminal clearance rate, k_t), the total body clearance (CL) is determined to be 27.1 ml•kg^{-1}min^{-1} [Berezhkovskiy 2013].

Tissue uptake and distribution of TLQP-21

We measured in the same animals the tissue uptake and distribution of the peripherally injected ^{125}I-TLQP-21. The pancreas and kidney have the greatest uptakes among all the tissues tested based on either tissue weight or tissue proteins (Table 1). Excluding the brain, all other organs assessed have a similar peptide uptake when this is normalized by tissue protein content (Table 1). As expected, the subcutaneous inguinal adipose tissue takes up the least amount of the peptide on a unit tissue weight basis. We also estimated the relative whole organ uptake by using weights from in-house data of the same breed rats (Table 1 for details). Using this estimate the relative uptake in the entire adipose organ is in par with kidney, liver, pancreas. Due to its large total mass skeletal muscle is a major site of systemic peptide uptake, whereas adrenal, heart and spleen are the smallest contributors on a whole organ basis. Importantly, our data demonstrate that peripherally injected TLQP-21 only minimally crosses the blood brain barrier. Indeed the uptake by cerebrum, cerebellum, hypothalamus and brain stem is insignificant (Table 1). Finally, we also measured the expressions of C3aR1 in six selected organs. The relative expression was largely consistent with the tissue uptake with the highest level being found in liver, adipose tissue and heart (Figure 2). Conversely, expression in the brain was lower when compared to the other organs, and expression in the skeletal muscle (gastrocnemius and tibialis anterior) was negligible (Figure 2).

Stability of TLQP-21 in mouse plasma

We incubated TLQP-21 in 100% mouse plasma and collected samples at 0, 10 and 60 min for LC-MS analysis. In line with the in vivo clearance study, the full length peptide was not identifiable after 10 minutes. However, several fragments, which represent the product of

proteolytic cleavage by prohormone convertase, could be identified (Table 2 and Figure 3). Interestingly, at 10 minutes the most enriched fragment was TLQPPASSRRRHFHHALPPA, suggesting that the C-terminal arginine is the first amino acid being cleaved by plasma peptidases. The presence of a large amount of HFHHALPPAR also suggests that the 3 arginines in the center of the peptide are also rapidly cleaved. At 60 minutes, all these fragments were undetectable and the only remaining fragments are represented by N-terminal hexa- and hepta-peptides as well as the HFHHALPPA situated between the triple arginine residues in the center of the peptide and the C-terminal arginine.

The effects of TLQP-21 on isoproterenol-stimulated lipolysis

Previous work established a critical role for TLQP-21 on enhancing βARs-induced lipolysis [Possenti et al., 2012; Ceroetal., 2014, 2017]. During isoproterenol infusion, plasma palmitate concentration was more than doubled (Figure 4a), then, it progressively diminished in the control group so that by the end of the experiment it is reduced to ~75% of the initial value. In contrast, plasma palmitate concentration was sustained for the entire experiment in the TLQP-21 treated group. As a result, there is a significant difference in plasma palmitate AUCs between the two groups (Figure 4b). As plasma FFA concentration is also affected by tissue uptake, the palmitate Ra (as measured with [U-^{13}C]palmitate), an one way process unaffected by uptake, was simultaneously determined. Palmitate Ra was 29% greater in the TLQP-21 treated group than that in the vehicle treated control group (Figure 4B). Therefore, the sustained plasma palmitate concentration in the treated group is a result of sustained lipolysis.

DISCUSSION

TLQP-21 has emerged as a novel therapeutic target with the potential for treating obesity primarily by modulating lipolysis without apparent adverse cardiovascular effects as assessed by studies in mice and rats [Possenti et al., 2012; Cero et al., 2017; Fargali et al., 2014]. So far, very little is known about its clearance kinetics in animal models. To our knowledge, the present study is the first characterizing the pharmacokinetics using ^{125}I-labeled peptide as an isotopic tracer in a rodent model as well as its plasma stability using mass spectrometry techniques.

The emphasis of the kinetic characterization is the initial and terminal phases of clearance after *i.v.* administration of the peptide as a single bolus injection. The initial phase represents unidirectional transfer from plasma to various tissues before subsequent reversal, or release from the tissues, as time elapses. The terminal phase is emphasized because it is relevant for understanding the steady state kinetics of the peptide and, for this reason, is discussed in greater detail. The terminal kinetic parameters k_t and $t_{1/2(t)}$ are used here for characterizing the clearance profile of TLQP-21. At 110 min of the *i.v.* dosing, $t_{1/2(t)}$ (terminal half-life) falls in a range often seen for various drugs when tested in rats. Typically, the half-lives for peptides are significantly shorter in rodents compared to humans [Löscher, 2007]. The observed short half-life in the present study occurs for several reasons. First, the dose used in our clearance study is small (<0.1 mg/kg). By comparison, many other pharmacokinetic studies in rats use doses that are several orders of magnitude greater, as much as 200 mg/kg

[Löscher, 2007]. Secondly, a single dose is used in the present study rather than multiple administrations daily. Importantly also, for some drugs the half-life is dose-dependent such as the case of 5,5-diphenyihydantoin [Gerber et al., 1971] and other peptides [Gros et al., 1990]. Collectively, considering these reasons we hypothesize that the peptides' half-life can be prolonged by using larger doses or/and administered more frequently. This, however, needs to be validated in future investigations. Daily peripheral injection of TLQP-21 for days to weeks, exerts a significant biological effect both acutely and chronically in mice, rats and hamsters (e.g. [Cero et al., 2017; Fargali et al., 2014; Stephens et al., 2012; Jethwa et al., 2007; Bartolomucci et al., 2006]). This suggests that the effective activation of downstream signaling occurs and persists even after a brief (due to rapid cleavage in plasma) peptide-mediated receptor activation. Alternatively, the injected synthetic peptide can elicit a feed-forward effect increasing endogenous release of TLQP-21 [Possenti et al., 2012] and/or, the receptor activation can modulate long term gene programming and physiological functions in target cells with mechanisms that are only starting to emerge [Stephens et al., 2012; Cero et al., 2017; Doleen et al., 2017].

The corrected initial half-life $t_{1/2(t)}$, of 0.97 min suggests that TLQP-21 rapidly penetrates the plasma membrane and, as our *in vitro* plasma stability data suggest, is quickly cleaved by proteases. The apparent rapid cross-membrane transport that we observed is consistent with high receptor affinity, a common attribute of most peptide-based endogenous agonists. The information on the initial phase clearance may be of significance for designing future studies. On the other hand, our *in vitro* data demonstrate that similar to other neuropeptides [Kostelnik et al., 2015; Gros et al., 1990; Cianflone et al. 2003], TLQP-21 is rapidly degraded in plasma, leading to a number of fragments. This finding is not surprising considering that the test peptide is in a native form that has yet to be optimized. These observations provide information that will be useful in guiding the development of chemical refinements. The cleavage sites are diverse, including a triplet of positively charged Arg-residues, a C-terminal arginine, three histidines and a hydrophobic leucine residue. The major fragment found to be enriched at 10 minutes is a 20 amino acid-long peptide devoid of the C-terminal arginine. Based on reported biological results, this fragment is inactive at the C3aRl [Cero et al., 2014; Doleen et al., 2017]. Serum carboxypeptidase rapidly regulates the activity of C3a, the first identified ligand for the C3aRl, by cleaving the C-terminal arginine residue (R77), generating a des-arginine peptide (also known as acylation stimulated protein, ASP), which is inactive at C3aRl [Cianflone et al., 2003; Murray et al., 2000]. Similar to C3a, the receptor activation residues are located at the very C-terminus of TLQP-21 [Cero et al., 2014], By mutating the Arg21 into Arg21 (R21A peptide) the resulting peptide is inactive [Cero et al., 2014, 2017; Doleen et al., 2017] that still preserves its ability to form α-heli*x* in the presence of the C3aRl [Cero et al., 2014], To date, the putative TLQP des-Arg21 peptide has yet to be identified *in vivo* [Bartolomucci et al., 2006]. Overall, these results suggest that plasma peptidases degrade the native TLQP-21 to generate multiple smaller fragments that are unlikely to be biologically active [Cero et al., 2017; Petrocchi-Passeri et al., 2015] but rather limit its biological actions. Therefore, structural optimization of the peptide would likely increase its stability, as well as enhance and extend its biological activities. Furthermore, it suggests that the reported *in vivo* activities may represent but a mere fraction of what is possible, once suitable the optimized form. On the other hand,

because sustained lipolysis can lead to unwanted metabolic effects such as ectopic lipid deposition and lipotoxicity, the medicinal refinement may have to strike a balance between sustained agonistic potency with intermittent pauses to minimize toxicity and maximize safety. The relative tissue distribution profile of *i.v.* injected TLQP-21 differs when expressed as unit weight as compared to that based on whole organ mass. This difference is expected given the differences in organ sizes. However, the absolute distributions based on tissue proteins are similar among the organs studied, although the pancreas and kidney are higher than average, and the brain is the lowest. Interestingly, adipose tissue is quite unique. It is an insignificant site of uptake by unit tissue weight but comparable to other organs when expressed in terms of tissue proteins. This discrepancy can be explained, at least partially, by the low protein content and high lipid content (~90% of its weight is from the large single intracellular lipid droplet) of adipose tissue. With respect to its effect on lipolysis, however, uptake in relation to tissue protein is more relevant as its actions rely on presence in the cell membrane where most of its proteins reside. The high abundance of TLQP-21 in the cell membrane compartment [Possenti et al., 2012] supports its ability to influence adipocyte lipolysis and is consistent with the high peptide-receptor binding activity in this tissue. Skeletal muscle also differs in relative uptake of the peptide, as the greatest due to its huge mass but similar to other tissues in terms of tissue protein. Because FFA release from muscle is thought to be negligible [Evans et al., 2002], and because the expression of the TLQP-21 receptor C3aR1 in the skeletal muscle (GN and TA) was minimal, it is unlikely that this tissue would be a contributor to the increase in systemic lipolysis produced by the peptide. It is possible, however, that TLQP-21 could influence lipolysis of intramyocellular triglycerides, a major energy storage for the tissue [Guo, 2001], and thus influence fuel selection in muscle. The precise function of TLQP-21 in myocytes remains to be clarified in additional studies.

The tissue distribution of *i.v.* injected ^{125}I-TLQP-21 (Table 1), the ligand-receptor binding (mice membrane system [Possenti et al., 2012] and the C3aR1 expression (Fig. 2) are largely overlapping in adipose tissue but not other organs. Once again, this supports the adipose tissue as the most prominent target for actions of the peptide. In contrast, skeletal muscle has negligible C3aR1 expression and low ligand-receptor binding with a finite amount of *in vivo* peptide uptake. This suggests that the peptide uptake by this tissue may be a function of non-specific binding or simply a methodological artifact.

Like muscle, the liver does not appear to be a source of circulating FFA [Nelson et al., 2007]. Although the liver displays the highest C3aRl expression, it has the lowest ligand-receptor binding; this suggests that TLQP-21 would have minimal influence on lipolys is of hepatic intracellular triglyceride. Unfortunately, the heart, which also contains intracellular triglycerides as a primary energy source, has not been tested for ligand-receptor biding. However, its relatively small amounts of peptide uptake suggest that it is not a source of the plasma FFA. While the brain is an important target for TLQP-21 based on ligand-receptor binding activity [Possenti et al., 2012], our data now demonstrate that when the peptide is peripherally injected, it does not cross the blood brain barrier. This finding has important implication and suggests that the anti-obesity effect exerted by central [Bartolomucci et al., 2006] and peripheral [Cero et al., 2014] TLQP-21 injection are mediated by different mechanisms [Jiang et al, 2017].

Finally, TLQP-21 is taken up avidly by the pancreas, kidney and adrenals. TLQP-21 influences both exocrine [Petrella et al, 2012] and endocrine [Stephens et al, 2012, 2017;] pancreatic function, and VGF is highly expressed in these organs. Because of limited information about the peptide's effect in these particular organs, it is premature to speculate on the significance of the peptide uptake results presented herein. Rather, the results may suggest that these organs could be important targets for this neuropeptide and thus worth additional investigations.

The pro-lipolytic property of TLQP-21 has been previously reported [Possenti et al, 2012; Cero et al., 2017], The increased plasma palmitate concentration is maintained for at least 60 min in rats treated with isoproterenol and the peptide. In contrast, in the control rats treated with isoproterenol alone, plasma FFA concentration progressively decreased soon after an initial spike [Divertie et al, 2003]. One limitation of that study is that it is not known whether the sustained plasma FFA concentration is a result of continue lipolysis alone or also contributed by suppressed FFA uptake. Either or both can result in increased plasma FFA concentration. The data presented herein clarifies this question by showing that the increased plasma FFA concentration is attributable to increased Ra of FFA (i.e. lipolysis) in the peptide treated rats (Fig. 4A, Fig. 4B). Therefore, the pro-lipolytic property of TLQP-21 is confirmed in this study. However, it is important to determine whether the peptide also alters FFA uptake that would contribute to defining its metabolic profile and may relate to its safety profile for therapeutic purposes. For instance, if it suppresses FFA uptake by skeletal muscle or the heart, its therapeutic use could provide additional benefits in the treatment of obesity and type 2 diabetes. In these populations the well-known metabolic inflexibility (insulin resistance) of skeletal muscle (i.e. non-suppressible lipid utilization prandially) is a key component of the metabolic syndrome. In the heart, elevated lipid oxidation is believed to cause myocardial toxicity. Thus, suppressing FFA uptake could ameliorate these conditions. Ultimately, the effects of augmentation of lipolysis and suppression of FFA uptake and/or utilization by skeletal muscle would depend on the influence of these changes on energy balance. In brief, the *in vivo* data obtained in rats have unambiguously demonstrated that TLQP-21 increases lipolysis by potentiating the β-AR system. Meanwhile, the results also generated new questions that require additional studies in order to more completely understand the therapeutic use and metabolic consequences of this novel peptide agonist.

In summary, the present study for the first time characterized the pharmacokinetics and plasma stability of native TLQP-21 peptide. Its *in vivo* half-life is found to be relatively short following a small, acute bolus injection. In addition, the plasma stability data demonstrate a rapid and sequential cleavage of the four arginine residues which provide important insights for chemical refinement aimed at improving its stability and efficacy. Finally, our results support the hypothesis that TLQP-21 acts on adipose tissue to promote lipolysis and, therefore, potentially a future medication for obesity therapies by reducing body fat.

Supplementary Material

Refer to Web version on PubMed Central for supplementary material.

ACKNOWLEDGEMENTS

Supported by R01DK102496 by NIH, and Decade of Discovery in Diabetes Grant, Minnesota Partnership for Biotechnology and Medical Genomic to A.B, and RO1 HL67933 to J.M.

REFERENCES

Adam A, Leclair P, Montpas N, Koumbadinga GA, Bachelard H, Marceau F. Altered cardiac bradykinin metabolism in experimental diabetes caused by the variations of angiotensin-converting enzyme and other peptidases. Neuropeptides. 2010;44(2):69–75. [PubMed: 19836835]

Aguilar E, Pineda R, Gaytan F, Sanchez-Garrido MA, Romero M, Romero-Ruiz A, Ruiz-Pino F, Tena-Sempere M, Pinilla L. (2013) Characterization of the reproductive effects of the Vgf-derived peptide TLQP-21 in female rats: in vivo and *in vitro* studies. Neuroendocrinology. 98(1):38–50. [PubMed: 23485923]

Bartolomucci A, La Corte G, Possenti R, Locatelli V, Rigamonti AE, Torsello A, Bresciani E, Bulgarelli I, Rizzi R, Pavone F, D'Amato FR, Severini C, Mignogna G, Giorgi A, Schinina ME, Elia G, Brancia C, Ferri GL, Conti R, Ciani B, Pascucci T, Dell'Omo G, Muller EE, Levi A, Moles A. (2006) TLQP-21, a VGF-derived peptide, increases energy expenditure and prevents the early phase of diet-induced obesity. Proc Natl Acad Sci U S A. 103(39):14584–9. [PubMed: 16983076]

Bartolomucci A, Possenti R, Mahata SK, Fischer-Colbrie R, Loh YP, Salton SR. (2011). The extended granin family: structure, function, and biomedical implications. Endocr Rev 32(6):755–97. [PubMed: 21862681]

Berezhkovskiy LM. (2013) On the accuracy of a one-compartment approach for determination of drug terminal half-life. J Pharm Sci. 102(7):2082–4. [PubMed: 23620272]

Berezhkovskiy LM. (2013b) Prediction of drug terminal half-life and terminal volume of distribution after intravenous dosing based on drug clearance, steady-state volume of distribution, and physiological parameters of the body. J Pharm Sci. 102(2):761–71. [PubMed: 23233148]

Cassina V, Torsello A, Tempestini A, Salerno D, Brogioli D, Tamiazzo L, Bresciani E, Martinez J, Fehrentz JA, Verdie P, Omeljaniuk RJ, Possenti R, Rizzi L, Locatelli V, Mantegazza F (2013). Biophysical characterization of a binding site for TLQP-21, a naturally occurring peptide which induces resistance to obesity. Biochim Biophys Acta. 1828(2):455–60. [PubMed: 23122777]

Cero C, Razzoli M, Han R, Sahu BS, Patricelli J, Guo ZK, Zaidman NA, Miles JM, O'Grady SM, Bartolomucci A. (2017) The neuropeptide TLQP-21 opposes obesity via C3aR1-mediated enhancement of adrenergic-induced lipolysis. Mol Metabol. 6(1):148–158.

Cero C, Vostrikov VV, Verardi R, Severini C, Gopinath T, Braun PD, Sassano MF, Gurney A, Roth BL, Vulchanova L, Possenti R, Veglia G, Bartolomucci A. (2014) The TLQP-21 peptide activates the G-protein-coupled receptor C3aR1 via a folding-upon-binding mechanism. Structure. 22(12): 1744–53. [PubMed: 25456411]

Choi YH, Lee I, Lee MG. (2010). Slower clearance of intravenous metformin in rats with acute renal failure induced by uranyl nitrate: Contribution of slower renal and non-renal clearances. Eur J Pharm Sci. 39(1–3):1–7. [PubMed: 19454315]

Cianflone K, Xia Z, Chen LY. (2003) Critical review of acylation-stimulating protein physiology in humans and rodents. Biochimica et Biophysica Acta. 1609(2):127–143. [PubMed: 12543373]

Davies B, and Morris T. (1993) Physiological parameters in laboratory animals and humans. Pharm Res. 10(7):1093–5. [PubMed: 8378254]

Divertie G, Jensen MD, Cryer P. Miles JM(2003) Lipolytic responsiveness to epinephrine in nondiabetic and diabetic humans. Am J Physiol 272:E1130–E1135.

Dole VP. (1956) A relation between non-esterified fatty acids in plasma and the metabolism of glucose. J. Clin Invest. 35: 150–154. [PubMed: 13286333]

Doolen S, Cook J, Riedl M, Kitto K, Kohsaka S, Honda CN, Fairbanks CA, Taylor BK, Vulchanova L. (2017) Complement 3a receptor in dorsal horn microglia mediates pronociceptive neuropeptide signaling. Glia. 65:1976–1989. [PubMed: 28850719]

Evans K,Burdge GC, Wootton SA, Clark ML, Frayn KN (2002) Regulation of dietary fatty acid entrapment in subcutaneous adipose tissue and skeletal muscle. Diabetes 51:2684–2690. [PubMed: 12196459]

Fairbanks CA, Peterson CD, Speltz RH, Riedl MS, Kitto KF, Dykstra JA, Braun PD, Sadahiro M, Salton SR, Vulchanova L. (2014) The VGF-derived peptide TLQP-21 contributes to inflammatory and nerve injury-induced hypersensitivity. Pain. 155(7)1229–37. [PubMed: 24657450]

Fargali S, Garcia AL, Sadahiro M, Jiang C, Janssen WG, Lin WJ, Cogliani V, Elste A, Mortillo S, Cero C, Veitenheimer B, Graiani G, Pasinetti GM, Mahata SK, Osborn JW, Huntley GW, Phillips GR, Benson DL, Bartolomucci A, Salton SR. (2014) The granin VGF promotes genesis of secretory vesicles, and regulates circulating catecholamine levels and blood pressure. FASEBJ. 28(5)2120–33.

Gerber N, Weller WL, Lynn R, Rangno RE, Sweetman BJ, Bush MT. (1971) Study of dose-dependent metabolism of 5,5-diphenyl-hydantoin in the rat using new methodology for isolation and quantitation of metabolites in vivo and *in vitro*. J Pharmacol Exp Ther. 178(3):567–79. [PubMed: 5571905]

Gros C, Souque A, Schwartz JC. Degradation of atrial natriuretic factor in mouse blood in vitro and in vivo: role of enkephalinase. Neuropeptides. 1990;17(l):l–5.

Guo ZK, Nielsen S, Burguera B, Jensen MD. (1997) Free fatty acid turnover measured using ultralow doses of [U-13C]palmitate. J Lipid Res. 38(9)1888–95. [PubMed: 9323598]

Guo ZK, Zhou L. (2003) Dual tail catheters for infusion and sampling in rats as an efficient platform for metabolic experiments. Lab Animal (NY). 32(2):45–8.

Guo ZK. (2001) Triglyceride content in skeletal muscle: variability and the source. Anal Biochem. 296(1)1–8. [PubMed: 11520026]

Hannedouche S, Beck V, Leighton-Davies J, Beibel M, Roma G, Oakeley EJ, Lannoy V, Bernard J, Hamon J, Barbieri S, Preuss I, Lasbennes MC, Sailer AW, Suply T, Seuwen K, Parker CN, Bassilana F (2013). Identification of the C3a receptor (C3AR1) as the target of the VGF-derived peptide TLQP-21 in rodent cells. JBiol Chem. 288(38):27434–43. [PubMed: 23940034]

Holliday MA, Potter D, Jarrah A, Bearg S. (1967) The relation of metabolic rate to body weight and organ size. Pediatr Res. 1967 1(3)185–95. [PubMed: 4965967]

Jethwa AW, Nilaweera KN, Brameld JM, Keyte JW, Carter WJ, Bolton N, Bruggraber M, Morgan PJ, Barrett P, Ebling FJP. (2007) VGF-Derived Peptide, TLQP-21, Regulates Food Intake and Body Weight in Siberian Hamsters. Endocrinology. 148: 4044–4055. [PubMed: 17463057]

Jiang C, Lin WJ, Sadahiro M, Shin AC, Buettner C, Salton SR. Embryonic ablation of neuronal VGF increases energy expenditure and reduces body weight. Neuropeptides. 2017;64:75–83. [PubMed: 28024880]

Kostelnik KB, Els-Heindl S, Kloting N, Baumann S, von Bergen M, Beck-Sickinger AG. High metabolic in vivo stability and bioavailability of a palmitoylated ghrelin receptor ligand assessed by mass spectrometry. Bioorg Med Chem. 2015;23(14):3925–32. [PubMed: 25541202]

Löscher W (2007) The pharmacokinetics of antiepileptic drugs in rats: consequences for maintaining effective drug levels during prolonged drug administration in rat models of epilepsy. Epilepsia. 48(7)1245–58. [PubMed: 17441999]

Molteni L, Rizzi L, Bresciani E, Possenti R, Petrocchi Passeri P, Ghè C, Muccioli G, Fehrentz JA, Verdie P, Martinez J, Omeljaniuk RJ, Biagini G, Binda A, Rivolta I, Locatelli V, Torsello A (2017). Pharmacological and Biochemical Characterization of TLQP-21 Activation of a Binding Site on CHO Cells. Front Pharmacol 30;8:167.

Murray I, Havel PJ, Sniderman AD, Cianflone K. (2000) Reduced body weight, adipose tissue, and leptin levels despite increased energy intake in female mice lacking acylation-stimulating protein. Endocrinology. 141(3)1041–1049. [PubMed: 10698180]

Nelson RH, Edgerton DS, Basu R, Roesner JC, Cherrington AD, Miles JM (2007). Triglyceride uptake and lipoprotein lipase-generated fatty acid spillover in the splanchnic bed of dogs. Diabetes 56:1850– 55. [PubMed: 17416801]

Petrella C, Broccardo M, Possenti R, Severini C, Improta G (2012) TLQP-21, a VGF-derived peptide, stimulates exocrine pancreatic secretion in the rat. Peptides. 36(1)133–6. [PubMed: 22561241]

Petrocchi-Passeri P, Cero C, Cutarelli A, Frank C, Severini C, Bartolomucci A, Possenti R. (2015) The VGF-derived peptide TLQP-62 modulates insulin secretion and glucose homeostasis. J Mol Endocrinol. 54(3):227–39. [PubMed: 25917832]

Piao Y, Liu Y, Xie X (2013) Change trends of organ weight background data in Sprague Dawley rats at different ages. J Toxicol Pathol. 26(l):29–34. [PubMed: 23723565]

Possenti R, Muccioli G, Petrocchi P, Cero C, Cabassi A, Vulchanova L, Riedl MS, Manieri M, Frontini A, Giordano A, Cinti S, Govoni P, Graiani G, Quaini F, Ghe C, Bresciani E, Bulgarelli I, Torsello A, Locatelli V, Sanghez V, Larsen BD, Petersen JS,Palanza P, Parmigiani S, Moles A, Levi A, Bartolomucci A (2012). Characterization of a novel peripheral pro-lipolytic mechanism in mice: role of VGF-derived peptide TLQP-21. BiochemJ. 441(l):511–22. [PubMed: 21880012]

Razzoli M, Bo E, Pascucci T, Pavone F, D'Amato FR, Cero C, Sanghez V, Dadomo H, Palanza P, Parmigiani S, Ceresini G, Puglisi-Allegra S, Porta M, Panzica GC, Moles A, Possenti R, Bartolomucci A. (2012) Implication of the VGF-derived peptide TLQP-21 in mouse acute and chronic stress responses. Behav Brain Res. 229(2):333–9. [PubMed: 22289198]

Reaven EP, Curry DL, Reaven GM (1987) Effect of age and sex on rat endocrine pancreas. Diabetes. 36(12): 1397–400. [PubMed: 3315787]

Rizzi R, Bartolomucci A, Moles A, D'Amato F, Sacerdote P, Levi A, La Corte G, Ciotti MT, Possenti R, Pavone F. (2008) The VGF-derived peptide TLQP-21: a new modulatory peptide for inflammatory pain. Neurosci Lett. 441(1)129–33. [PubMed: 18586396]

Severini C, La Corte G, Improta G, Broccardo M, Agostini S, Petrella C, Sibilia V, Pagani F, Guidobono F, Bulgarelli I, Ferri GL, Brancia C, Rinaldi AM, Levi A, Possenti R. (2009) *In vitro* and in vivo pharmacological role of TLQP-21, a VGF-derived peptide, in the regulation of rat gastric motor functions. Br J Pharmacol. 157(6):984–93. [PubMed: 19466987]

Stephens SB, Edwards RJ, Sadahiro M, Lin WJ, Jiang C, Salton SR, Newgard CB. (2017) The Prohormone VGF Regulates β Cell Function via Insulin Secretory Granule Biogenesis. Cell Rep. 20(10) :2480–2489. [PubMed: 28877479]

Stephens SB, Schisler JC, Hohmeier HE, An J, Sun AY, Pitt GS, Newgard CB. (2012) A VGF-derived peptide attenuates development of type 2 diabetes via enhancement of islet β -cell survival and function. Cell Metab.16(1):33–43. [PubMed: 22768837]

Trani E, Ciotti T, Rinaldi AM, Canu N, Ferri GL, Levi A, Possenti R. (1995). Tissue specific processing of the neuroendocrine protein VGF. J Neurochem. 65(6):2441–9. [PubMed: 7595538]

Wagner L, Kaestner F, Wolf R, Stiller H, Heiser U, Manhart S, Hoffmann T, Rahfeld JU, Demuth HU, Rothermundt M, von Horsten S. Identifying neuropeptide Y (NPY) as the main stress-related substrate of dipeptidyl peptidase 4 (DPP4) in blood circulation. Neuropeptides. 2016;57:21–34. [PubMed: 26988064]

Highlights

- i.v.-injected [^{125}I]TLQP-21 had an initial half-life of 0.97 minutes and a terminal half-life of 110 minutes
- The total net uptake by adipose tissue was 4.4% of the entire i. v. -injected dose equivalent.
- Upon i.v.-injection, liver, pancreas and adrenal gland showed higher uptake, while uptake by the brain was negligible.
- TLQP-21 sustained isoproterenol-stimulated lipolysis *in vivo.*
- TLQP-21 was rapidly degraded producing severalN-terminal and central sequence fragments after 10 and 60 minutes in plasma *in vitro.*

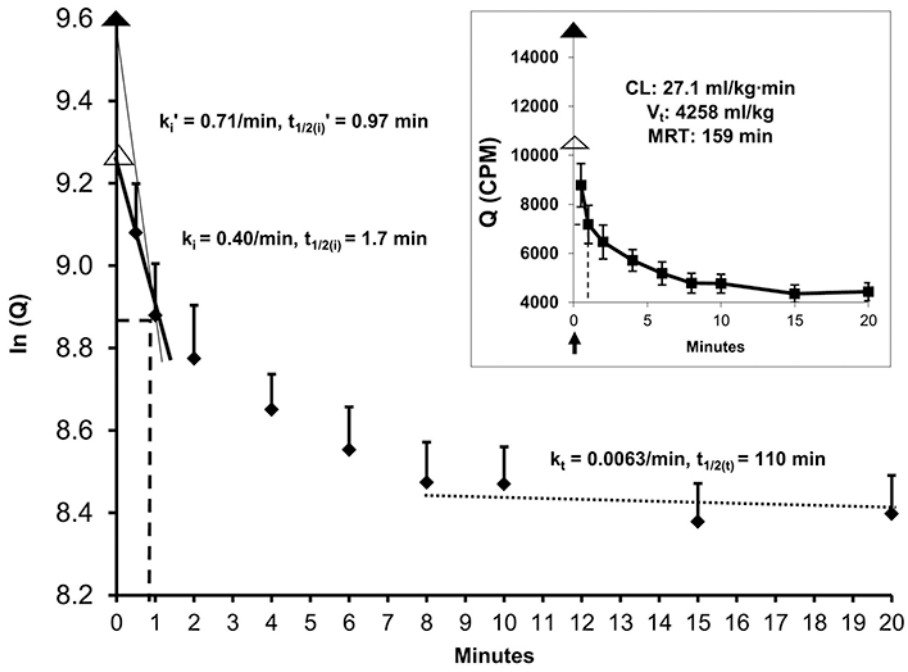

Figure 1.

Clearance kinetics of [^{125}I]TLQP-21 from plasma in rats (Sprague Dawley male, average body wt 400 g, n=7). ***Inset***: the observed data. At time 0, a dose of [^{125}I]TLQP-21 is injected via a tail vein (⬆), followed by arterial blood collections from 0.5 min on, as shown. Plasma is counted for ^{125}I-radioactivity in CPM/ml **(Q).** ***Main figure:*** data derived from the inset, **ln(Q),** for the calculation of the initialclearance rate constant, k_i (0.5–1 min, ▬), from which the theoretical maximum plasma radioactivity, **Q_0 (▲),** is extrapolated. The plasma volume of distribution (17.6 ml) as calculated from Q_0 is 41% greater than that expected for a 400 g rat (12.5 ml, or 3.12% of body wt [Davies, Morris 1993]), suggesting that Q_0 is underestimated. **Q_0'** (△), the corrected maximum plasma radioactivity based on this reported plasma volume of distribution, **k_i'**, the corrected initial clearance rate constant by incorporating **Q_0'** (0-**1** min, —). **k_t**, the terminal phase clearance rate constant (8–20 min,). The corresponding half-lives t1/2(i) , t1/2(i)' and t1/2(t) for k_i, k_i' and k_t, respectively, are calculated (ln2/k). The terminal phase is assumed based on the nearsteady clearance kinetics during the late phase (8–20 min,⋯) and is used as a single-compartment model to characterize the clearance kinetics of the peptide [Berezhkovskiy, 2013]. ***Symbols:***.----, graphically solved initial phase half-life that matched the calculated above. **V_t**, terminal volume of distribution [Berezhkovskiy, 2013b]. **CL,** total body clearance = ^{125}I-dose/$AUC_{Q0\text{-}726}$ (AUC, area under the curve, trapezoid method [Berezhkovskiy, 2013b]. **$AUC_{Q0\text{-}726}$** = $AUC_{Q0\text{-}20}$ + $AUC_{Q20\text{-}726}$, the latter is calculated from Q_{20} up to 726 min where 99% of the plasma ^{125}I-radioactivity is calculated to have been eliminated as predicted from k_t. **MRT,** mean residence time [Berezhkovskiy, 2013b].

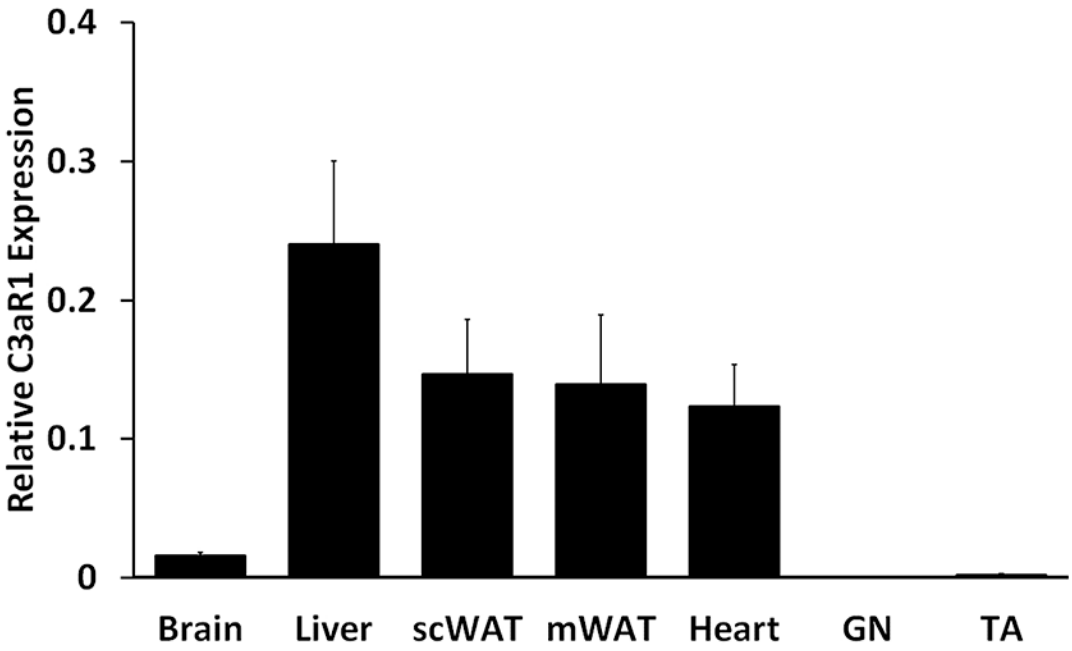

Figure 2:

Relative expression of C3aR1 (qPCR method) in rat brain, liver, subcutaneous white adipose tissue (scWAT), mesenteric white adipose tissue (mWAT), heart, gastrocnemius (GN) and tibialis anterior (TA). The expression is similar in liver, scWAT, MES and heart while significantly lower ($P<0.05$) in brain, and negligible in GN and TA muscle.

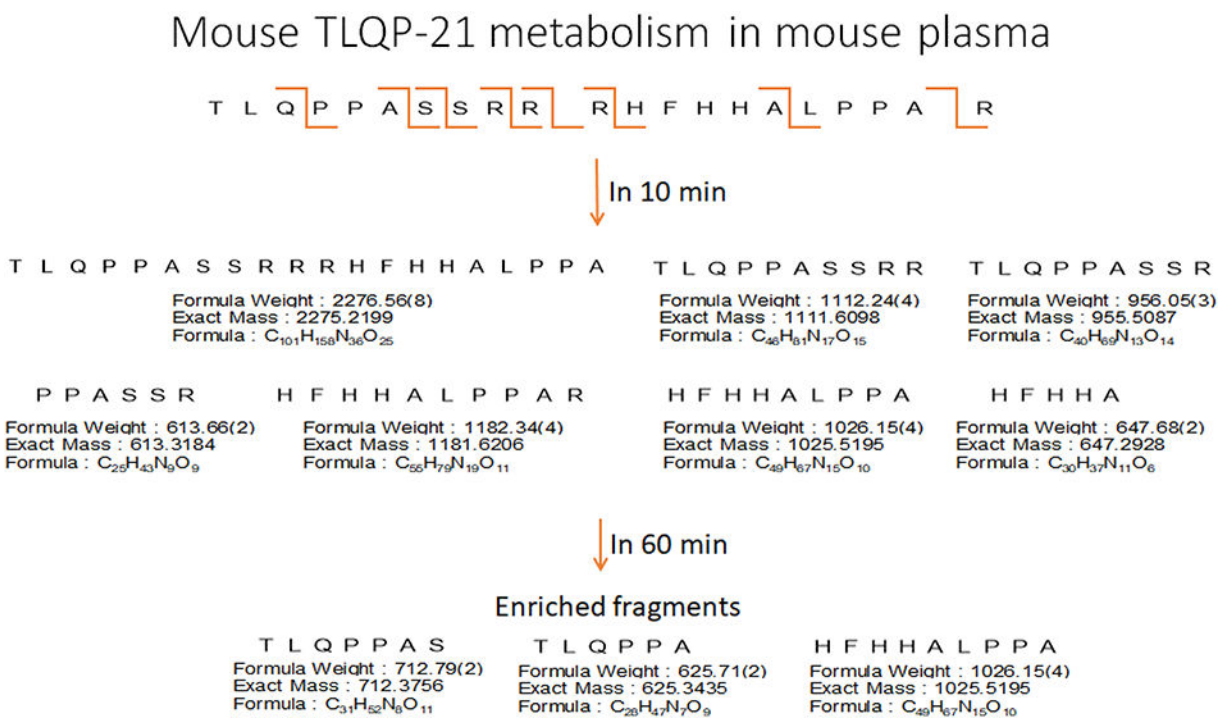

Figure 3.

TLQP-21 metabolism in mouse plasma assessed by LC-MS. Quantitative data are presented in Table 2. The figure shows the putative cleavage sites in the peptide's primary sequence (top) and the corresponding fragments identified at 10 and 60 minutes (bottom).

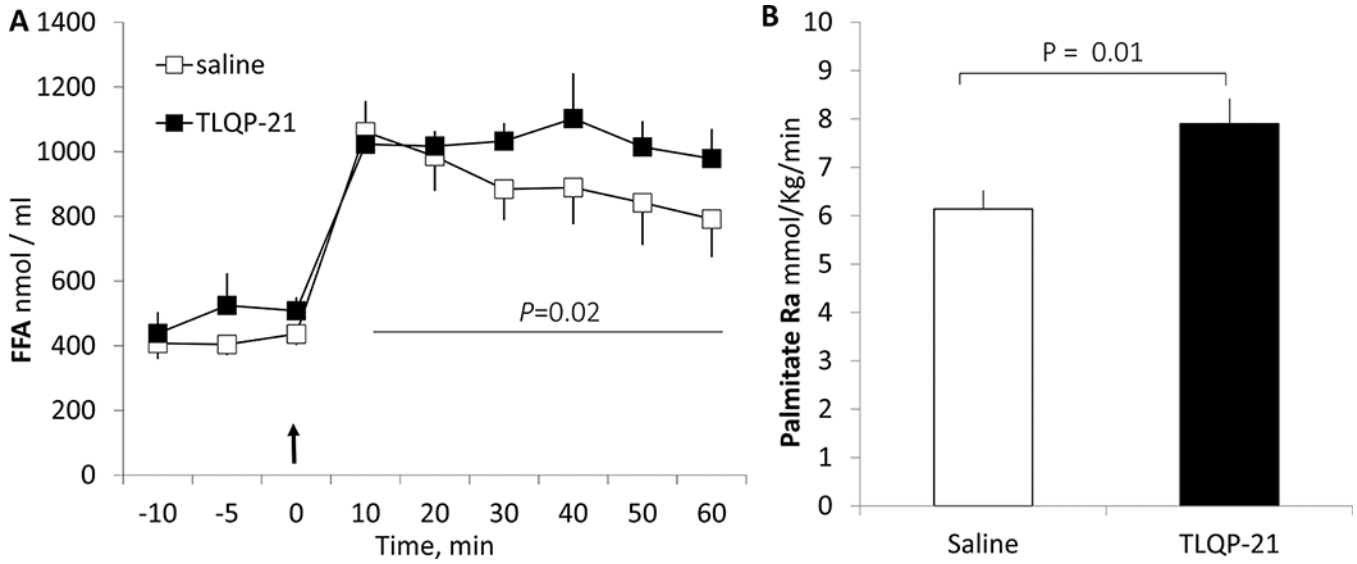

Figure 4.

The effects of TLQP-21 on plasma fatty acid concentration (A) and palmitate Ra (B) in normally fed rats infused with isoproterenol constantly. **A)** Isoproterenol infusion is started at 0 min (arrow) followed by a bolus injection of TLQP-21 or saline as control. *P*=0.02: comparison of AUC of plasma fatty acid concentrations between the groups. There is no statistical difference (P>0.05) over the basal period. **B)** Plasma palmitate Ra (micromole/kg $^{-1}$min^{-1}) during 10–60 min in the same experiments as A using [U-^{13}C] palmitate as a tracer. The baseline values are not shown (no statistically significant difference between the groups, P>0.05).

Table 1.

[^{125}I]TLQP-21 tissue distribution pattern in rats

	CPM	Relative tissue uptake	
Organs	**μg protein**	**g wet tissue* %**	**entire organ** %**
Pancreas	2.19±0.44	34.2±4.8	3.7
Kidney	1.22±0.12	27.3±3.0	6.4
Spleen	0.45±0.04	9.0±0.6	0.5
Liver	0.32±0.03	8.4±0.6	6.9
Heart	0.25±0.02	7.0±0.6	0.8
Adrenal Gland	0.35±0.02	6.8±0.7	0.03
ScWAT	0.28±0.03	1.5±0.1	4.4
Tibialis anterior	0.19±0.02	5.9±0.5	77
Cerebrum	0.07±0.02	<0.5	0.1
Cerebellum	0.08±0.02	<0.5	
Hypothalamus	0.06±0.01	<0.5	
Brain stem	0.06±0.01	<0.5	

*CPM/tissue (g) CPM/all tissues (g) x 100%.

**CP M/organ ÷ CPM/all organs x 100%.

scWAT, subcutaneous inguinal white adipose tissue. Organ weights are from in-house data of rats of the same breed. Total adipose tissue quantified by Rodent DEXA or from the published data for pancreas [Reaven et al., 1987], and kidney, spleen, liver, heart, adrenal gland and brain [Piao et al., 2013]. Skeletal muscle is assumed to be 40% of body weight [Holliday et al., 1967].

Table 2.

Observed masses and matched peptide fragments from mouse TLQP-21 during plasma stability study.

	Observed Mass	Matched Peptide Fragment	Residues	Relative abundance
10 minutes				
1	1139.1($M+2H^+$)/759.8($M+3H^+$)	TLQPPASSRRRHFHHALPPA	1–20	65%
2	1112.6($M+1H^+$)	TLQPPASSRR	1–10	*
3	956.2($M+1H^+$)	TLQPPASSR	1–9	*
4	614.4¡$M+1H^+$)	PPASSR	4–9	*
5	1182.6($M+1H^+$)	HFHHALPPAR	12–21	28%
6	1026.5($M+1H^+$)	HFHHALPPA	12–20	*
7	648.4($M+1H^+$)	HFHHA	12–16	*
60 minutes				
1	713.1($M+1H^+$)/735.4($M+Na^+$)	TLQPPAS	1–7	14%
2	626.5($M+1H^+$)/648.4($M+Na^+$)	TLQPPA	1–6	10%
3	1026.5($M+ 1H^+$)/1048.5($M+Na^+$)	HFHHALPPA	12–20	45%

* Individual relative abundance of these fragments cannot be definitively quantified from the chromatogram.